Absolute Rate Coefficient of the HCCO + NO Reaction over the Range $T = 297-802$ K

S. A. Carl,* Q. Sun, L. Vereecken, and J. Peeters

Department of Chemistry, University of Leuven, Celestijnenlaan 200F, B-3001 Leuven, Belgium

Received: November 12, 2001; In Final Form: October 3, 2002

The absolute rate coefficient of the gas-phase reaction HCCO + NO was experimentally determined for the first time over an extended temperature range, 297−802 K. HCCO radicals were generated by pulsed-laser photolysis of CH_2CO at 193 nm. Their subsequent decay, under pseudo-first-order conditions, was monitored in real time using a newly developed laser-photofragment/laser-induced fluorescence technique (Carl, S. A.; Sun, Q.; Peeters, J. *J. Chem. Phys.* **2000**, *114*, 10332) that involved pulsed-laser photodissociation of HCCO at 266 nm and laser-induced fluorescence at ca. 430 nm of the resulting nascent rotationally excited $CH(X^2\Pi)$ photofragment. The rate coefficient of the title reaction was found to exhibit a negative temperature dependence described by $k_5(T)_{(HCCO+NO)} = (1.6 \pm 0.2) \times 10^{-11} \exp(340 \pm 30\ K/T)$ cm^3 s^{-1} molecule^{-1} (2σ errors). In combination with the recent theoretically determined branching ratios for this reaction of this laboratory (Vereecken, L.; Sumathy, R.; Carl, S. A.; Peeters, J. *Chem. Phys. Lett.* **2001**, *344*, 400), the temperature dependencies of the two dominant product channels, HCN + CO_2 and HCNO + CO, may be described by $k_{5a} = (3.7 \pm 0.3) \times 10^{-10} T^{-0.72\pm0.02} \exp(200 \pm 30\ K/T)$ cm^3 s^{-1} molecule^{-1} and $k_{5b} = (1.4 \pm 0.2) \times 10^{-11} \exp(320 \pm 30\ K/T)$ cm^3 s^{-1} molecule^{-1}, respectively, where the given (2σ) error limits are derived from those of the present experimental work only.

1. Introduction

Several important phenomena of hydrocarbon combustion (ultraviolet[1] and visible[2,3] chemiluminescence, soot,[4−6] chemi-ions,[7,8] and both prompt formation[9] and removal[10−13] of nitric oxide) have a complex series of reactions at their root driven by small and highly reactive hydrocarbon radicals.[14] Of these reactions, those involving the ketenyl radical, HCCO, play a central role,[14] particularly the rapid reaction of ketenyl with atomic hydrogen,[15,16] which leads to highly reactive CH[17] and $CH_2(\tilde{a}^1A_1)$;[18]

$$HCCO + H \rightarrow CH_2(\tilde{a}^1A_1) + CO \quad (1a)$$

$$\rightarrow CH_2(\tilde{X}^3B_1) + CO \quad (1b)$$

$$CH_2(\tilde{a}^1A_1) + M \rightarrow CH_2(\tilde{X}^3B_1) + M \quad (2)$$

$$CH_2(\tilde{X}^3B_1) + H \rightarrow CH(X^2\Pi) + H_2 \quad (3)$$

These radicals are known to undergo rapid reactions with many hydrocarbons, notably C_2H_2,[19−22] leading to higher unsaturated hydrocarbons, which are the building blocks of polycyclic aromatic hydrocarbons.[23,24]

In combustion, HCCO is formed mainly by oxidation of ethyne,[25−29]

$$C_2H_2 + O \rightarrow HCCO + H \quad (k_{4a}/k_4 \cong 0.8:\ 285-2100\ K) \quad (4a)$$

$$\rightarrow CH_2 + CO \quad (k_{4b}/k_4 \cong 0.2:\ 285-2100\ K) \quad (4b)$$

and thought to be removed mainly by reaction with O_2, H, O, OH, and NO.

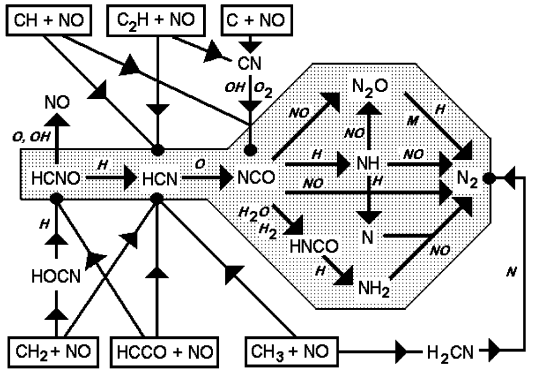

Figure 1. Reactions of small carbon-containing radicals with NO (including HCCO + NO) and their relationship to the NO-reburning reaction scheme (shaded area). A circle indicates the point of entry to the NO-reburning scheme for each boxed reaction. Several boxed reactions have two main product channels. Some product channels pass through an intermediate before entering the main scheme.

To date, several direct experimental studies have been published reporting the reactivity of HCCO with a variety of species. These studies, which encompass both relative- and absolute-rate determinations, have been reviewed recently by Carl et al.[30] Of concern to the present investigation is the reaction of HCCO with NO at elevated temperatures. This reaction has gained significant prominence in recent years due to its potential impact in reducing NO emissions of hydrocarbon combustion processes within the technology of "reburning".[31] In this context, experiments on laboratory[13] and pilot-scale[32] combustors show that injection of a hydrocarbon fuel above the main (NO-producing) combustion zone can significantly reduce the amount of emitted NO. Such experiments, together with detailed gas-phase reaction modeling[12,13,33,34] reveal that NO is removed by several series of gas-phase reactions that lead ultimately to the formation of N_2 (Figure 1). In each case,

* Corresponding author. E-mail: Shaun.Carl@chem.kuleuven.ac.be.

10.1021/jp014135i CCC: $22.00 © 2002 American Chemical Society
Published on Web 12/04/2002

nitric oxide removal begins with reaction of NO with a small carbon-containing radical: HCCO, C, CH, $CH_2(^3B_1)$, $CH_2(^1A_1)$, C_2H, or CH_3. Several intermediate steps, driven mainly by reactions involving O, H, and NO yield NH_i species ($i = 0-2$) and N_2O. Further reaction of NH_i with NO and reaction of N_2O with H, as well as decomposition of N_2O, leads finally to N_2.

On the basis of the present knowledge of the reactivity of these small hydrocarbon radicals, removal of NO by HCCO is thought to be prominent, and to dominate under many flame conditions, by virtue of the relatively large concentration of HCCO, its high reactivity toward NO,[10,35,36] and formation of HCN.[10,37−40]

$$\mathrm{HCCO + NO \rightarrow HCN + CO_2} \quad (5a)$$

$$\rightarrow \mathrm{HCNO + CO} \quad (5b)$$

$$\rightarrow \mathrm{HNC + CO_2} \quad (5c)$$

$$\rightarrow \mathrm{NCO + HCO} \quad (5d)$$

$$\rightarrow \text{other HCNO isomers + CO} \quad (5e)$$

As Figure 1 indicates, of the two dominant channels for this reaction, (5a) and (5b), a propensity to form HCN favors the propagation of the reaction series toward N_2, whereas formation of HCNO is thought to lead to recycling of NO via fast reaction of HCNO with OH and O.[39]

So far, only three experimental determinations of the rate constant of reaction 5 have been published; two of which are at room temperature only, the other is a relative rate determination. Unfried et al.[35] employed long-path, time-resolved, infrared absorption measurements on [HCCO] following its production by pulsed 193 nm laser photolysis of ketene. They reported an absolute rate constant of $k_5(298\ \mathrm{K}) = (3.9 \pm 0.5) \times 10^{-11}\ \mathrm{cm^3\ s^{-1}\ molecule^{-1}}$. A second room-temperature study was carried out by Temps et al.,[36] who generated HCCO in a fast flow system via reaction 4 and monitored its concentration−time (−distance) profile(s) using far infrared laser magnetic resonance. They obtained an absolute room-temperature rate constant for HCCO + NO of $k_5(298\ \mathrm{K}) = (2.2 \pm 0.7) \times 10^{-11}\ \mathrm{cm^3\ s^{-1}\ molecule^{-1}}$, almost a factor of 2 lower than that found by Unfried et al.[35] The only study of the temperature dependence of k_5 is a relative-rate determination by Boullart et al.[10] in which HCCO radicals were rapidly generated by reaction 4 in a flowing C_2H_2/O/H system. Given the fast competitive removal of HCCO by reaction with H and O atoms in this system, it was necessary to measure the rate coefficient of HCCO + NO relative to that of HCCO + O by monitoring the change in quasi-steady-state [HCCO] at a given reaction time as a function of added [NO]. From this study, the rate constant, k_5, was found to have a dependence on temperature given by $k_5(290-650\ \mathrm{K}) = (1.00 \pm 0.3) \times 10^{-11} \exp(-350 \pm 150\ \mathrm{K}/T)$, with a room-temperature value of $k_5(290\ \mathrm{K}) = (3.1 \pm 1.8) \times 10^{-11}\ \mathrm{cm^3\ s^{-1}\ molecule^{-1}}$. The latter room-temperature value, with its relatively broad error limits, encompasses the values of the two earlier measurements; thus a relatively large uncertainty remains. This uncertainty is even greater at the elevated temperatures of combustion due to both the error limits of this single, temperature-dependent study and its limited temperature range. There is thus an incentive for further measurement of $k_5(T)$ over a wide enough temperature range and with sufficiently high precision to allow more reliable extrapolations to combustion temperatures.

2. Experimental Methods

The experimental apparatus (Figure 2), experimental procedure, and our newly developed detection method for HCCO

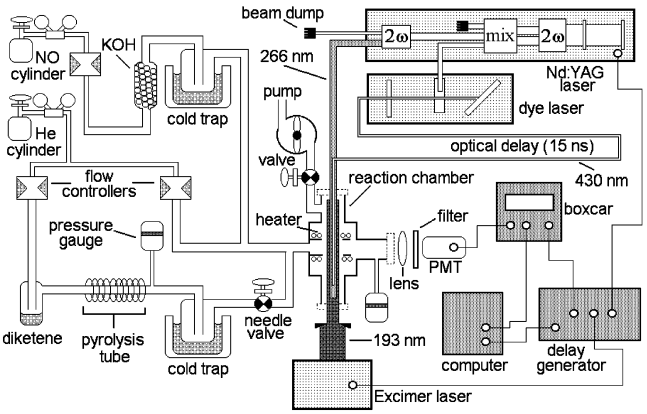

Figure 2. Experimental apparatus used for time-resolved measurements of [HCCO] detected by laser-photofragment (of HCCO)/laser-induced fluorescence (of nascent CH).

are described in detail elsewhere.[30] The principal points are repeated here.

HCCO radicals are generated by pulsed-laser (ArF excimer laser, 193 nm, ca. 10 mJ/pulse at 10 Hz) photolysis of ketene[16] along the central axis of a heatable, stainless steel reaction chamber.

$$\mathrm{CH_2CO} + 193\ \mathrm{nm}$$

$$\rightarrow \mathrm{HCCO}(\tilde{X}^2A'' \text{ and/or } \tilde{A}^2A') + \mathrm{H}(^1S) \quad (k_{6a}/k_6 = 0.11) \quad (6a)$$

$$\rightarrow \mathrm{CH_2}(\tilde{a}^1A_1) + \mathrm{CO} \quad (k_{6b}/k_6 = 0.19) \quad (6b)$$

$$\rightarrow \mathrm{CH_2}(\tilde{X}^3B_1) + \mathrm{CO} \quad (k_{6c}/k_6 = 0.63) \quad (6c)$$

$$\rightarrow \mathrm{C_2O}(\tilde{b}^1\Sigma^+) + \mathrm{H_2} \quad (k_{6d}/k_6 = 0.07) \quad (6d)$$

The indicated branching ratios are from ref 16.

A ceramic tube (99.7% Al_2O_3, with an internal, gray, oxidized SiC coating) inside the reaction chamber, which is surrounded by a Ni/Cr resistive wire, allows the gas mixture to be heated to temperatures of up to 900 K. The temperature of the gas in the small probed reaction volume is periodically monitored using a movable, calibrated chromel/alumel thermocouple. Spreads in the gas temperature range from ±1 K at 296 K to ±10 K at 802 K, our highest temperature kinetic measurements.

The reaction chamber is O-ring sealed at both ends by water-cooled (290 K) quartz windows that allow access for two pulsed photolysis laser beams and a pulsed probe laser beam. A third window, which is at right angles to the optical axis of the laser beams, allows imaging of fluorescence from the center of the reaction chamber.

The reaction chamber is connected to a throttled, rotary vacuum pump and a gas flow system allowing fresh, homogeneous gas mixtures of constant total pressure (typically 5.4 Torr) and known composition to continually pass. The gas mixture comprises ketene as the photolytic precursor of HCCO, the co-reactant, NO, and He. High-purity He (99.999%, Indugas) and NO (10.36% in helium, Praxair NV) are admitted to the flow system from their high-pressure cylinders via calibrated flow controllers (MKS Instruments Inc.). Possible NO_2 impurities in the NO/He cylinder are eliminated by flowing the NO/helium mixture through a tower of KOH pellets followed by a trap held at 195 K before entering the reaction chamber. Ketene on the other hand, is produced in situ, upstream of the reaction chamber, using a method similar to that employed by Unfried

et al.,[35] i.e., by pyrolysis of diketene vapor (the liquid-phase of 98% purity is stabilized by copper sulfate, Aldrich Chemical Corp.) in He at 800 K. A 195 K trap situated immediately downstream of the pyrolysis tube is used to collect any undissociated diketene before the gas enters the reaction chamber. The typical concentration of ketene in the reaction chamber is calculated to be about 5×10^{15} molecule cm^{-3}.

Concentrations of the co-reactant [NO] are accurately determined using the total reactor pressure, measured using a 0−10 Torr Barocel pressure sensor (Datametrics), and partial flow rates, measured using calibrated mass flow controllers (MKS Instruments Inc.). Total flow rates through the reactor are typically 150 sccm (cm^3 min^{-1} if at STP), which is sufficiently fast to replenish the active reaction volume in the 0.1 s period between successive excimer laser pulses, but still slow enough to be effectively static over HCCO (1/e) reaction lifetimes, which range from 14 to 200 μs.

Time-resolved measurements of the decreasing HCCO concentration, following process 6a, is achieved using a novel "laser-photofragment/laser-induced fluorescence" technique (LPF-LIF) in which the first probe laser pulse (266 nm) photodissociates HCCO, yielding CH(X) + CO, and a second probe laser pulse (430 nm), delayed by only a few nanoseconds, excites the A ← X transition in the CH photofragment, thus inducing CH fluorescence, the intenstiy of which is proportional [HCCO].[30]

Photodissociation of HCCO at 266 nm leads mainly to CH(X)[41]

$$\mathrm{HCCO} + h\nu\ (266\ \mathrm{nm}) \rightarrow \mathrm{CH}(\mathrm{X},\nu''=0,N''\leq 28) + \mathrm{CO} \quad (7)$$

The possible concurrent production of electronically excited $CH(^4\Sigma^+)$ is of no concern to the present measurements. Our recent work[30] demonstrates that nascent CH photofragments resulting from process 7 exhibit a highly excited rotational population distribution (up to $N'' = 28$) and are therefore easily distinguished from any chemically produced CH, which possess a Boltzmann rotational distribution with a population maximum at $N'' = 3$ at 298 K and $N'' = 5$ at 800 K. Therefore, the wavelength of the CH(A←X) probe laser pulse is tuned to excite only a highly rotationally excited state ($N'' = 13$ or 15, Q-branch):

$$\mathrm{CH}(\mathrm{X}^2\Pi,\nu''=0,N''=13\ \text{or}\ 15) + h\nu\ (430.35\ \text{or}\ 430.00\ \mathrm{nm}) \rightarrow \mathrm{CH}(\mathrm{A}^2\Delta,\nu''=0) \quad (8a)$$

$$\mathrm{CH}(\mathrm{A}^2\Delta) \rightarrow \mathrm{CH}(\mathrm{X}^2\Pi) + h\nu\ (\text{ca. } 430\ \mathrm{nm}) \quad (8b)$$

Probe laser absorption from thermally populated $N'' = 13$ and 15 levels of CH(X) produced by chemical reaction is insignificant under our experimental conditions below a reactor temperatures of about 600 and 1000 K, respectively. Nevertheless, effective discrimination of photofragment CH radicals requires that the time delay between (7) and (8a) be short enough that no significant rotational relaxation occurs. Such a short time delay, of ca. 16 ns, is achieved simply by introducing an optical path difference of 5 m between the HCCO photoysis pulse (Nd:YAG 4ω, 10 Hz) and the CH fragment excitation pulse (Nd:YAG/dye; ca. 430 nm, 10 Hz).

The fraction of ketene, lying along the laser path, dissociated to HCCO is calculated to be about 8×10^{-4} on the basis of a molecular absorption cross-section[42] of $\sigma_{(\text{ketene at } 193\ \mathrm{nm})} = 8 \times 10^{-19}$ cm^2 and a quantum yield for dissociation to HCCO of 0.11.[16] In the presence of excess [NO] (80 < [NO]/[HCCO] < 1500), [HCCO] observes pseudo-first-order kinetics with reaction (1/e) lifetimes ranging from about 14 to 200 μs. Note that under the conditions of the kinetic experiments, at $p = 5.4$ Torr (He), the two Renner−Teller states of HCCO are expected to be always equilibriated; in 10 μs, an HCCO radical undergoes about 1000 collisions with the He bath gas.

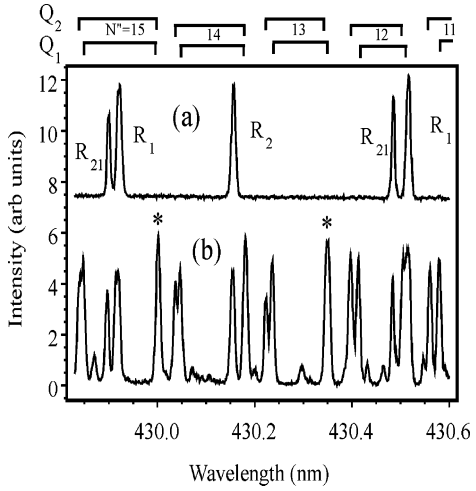

Figure 3. Portion of a room-temperature laser-excitation spectrum of CH near those transitions used for kinetic measurements (each marked with an asterisk): (a) a baseline shifted spectrum in the *absence* of the 266 nm, HCCO dissociation pulse, showing only low-*N*, R-branch transitions, (b) including high-*N*, Q-branch transitions arising from photodisociation of HCCO at 266 nm.

Optical emissions (CH(A→X)) from the center of the reaction chamber pass through the third window and are imaged onto a photomultiplier tube (PMT) (R955, Hamamatsu) fitted with a band-pass filter (430 nm ± 10 nm (fwhh), Oriel 59295). The PMT photocurrent, resulting from the temporal CH fluorescence, is voltage-converted and passed to a boxcar for integration (gate width = 1 μs, SR250, Stanford Research Systems). The result of this integration (a dc voltage) is collected as a single data point on a computer using an A/D converter (National Instruments).

Exponential decay profiles of [HCCO] are collected pulse-wise and are slowly constructed over a few hundred seconds by incrementing the time delay between the excimer laser pulse and the HCCO probe beam pulse every 10 excimer laser pulses, i.e., after 1 s each time. Triggering and precision timing (to 0.1 μs resolution) of the excimer and Nd:YAG fundamental pulses, as well as the Boxcar gate, is accomplished using a homemade, computer-controlled pulse generator.[43]

3. Results and Discussion

Figure 3 shows a rotationally resolved laser-excitation spectrum, $CH(A^2\Delta) \leftarrow CH(X^2\Pi)$, in the region encompassing the two spectral lines used to determine relative $[HCCO]_t$ profiles. For temperatures up to and including 600 K the $N'' = 13$ (430.35 nm, vacuum) line was used, for all other experimental temperatures $N'' = 15$ (430.00 nm, vacuum) was used. The figure clearly shows that in the absence of the 266 nm HCCO dissociation pulse only thermally populated CH remains. This chemically produced CH is in a quasi-steady-state governed by the reactions $CH_2 + H \rightarrow CH + H_2$ and $CH + CH_2CO \rightarrow$ products.

In the presence of an excess concentration of NO the time profile of [HCCO] should take the following simple exponential form:

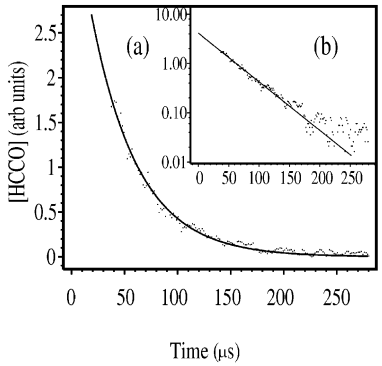

Figure 4. (a) Experimental time profile of [HCCO] (fitted to a single-exponential function) following 193 nm dissociation of CH_2CO (time = 0) in the presence of an NO concentration of 2.65×10^{14} molecule cm^{-3} and at a reactor temperature of 345 K. (b) Same profile displayed with a logarithmic *y* axis.

$$\frac{[\mathrm{HCCO}]_t}{[\mathrm{HCCO}]_0} = \exp(-(k_5' + \sum k_i[\mathrm{X}_i])t) \qquad \text{(i)}$$

where $k_5' = k_5[\mathrm{NO}]$ and $\sum k_i[\mathrm{X}_i]$ represents removal of HCCO by secondary reactions involving species X_i, having a rate constant k_i. Diffusion out of the observation region at the pressures and temperatures of the experiments is negligibly slow compared to reactive removal. For the present experiments, the simple exponential form of eq i is valid because the first constant term of the argument of the exponential function dominates the second time-dependent term, which, as discussed later, is mainly due to reaction of HCCO with H atoms.

Figure 4 shows an example time profile of [HCCO] obtained from nascent photofragment LIF of CH at 430 ± 10 nm following its initial excitation at 430.35 nm (from $N'' = 13$) or 430.00 nm ($N'' = 15$) in the presence of excess [NO] at 345 K. All decays measured in the presence of NO exhibit the expected exponential behavior described by eq i over the whole signal range between 2 and 2.5 orders of magnitude, as indicated by the weighted least-squares fit. In the absence of NO, HCCO is removed mainly by H atoms, coproduced in the photolysis of CH_2CO. Indeed, these profiles show a mixture of second- and first-order kinetics.

As explained in our recent publication,[30] HCCO time profiles could not be recorded at reaction times of less than about 20 μs because of interference from spontaneous emission from CH(A) produced directly by two-photon photolysis of CH_2CO at 193 nm.

$$\mathrm{CH_2CO} + 2h\nu\ (193\ \mathrm{nm}) \rightarrow \mathrm{CH}(\mathrm{A}^2\Delta) + \text{products} \qquad (9)$$

$$\mathrm{CH}(\mathrm{A}^2\Delta) \rightarrow \mathrm{CH}(\mathrm{X}^2\Pi) + h\nu\ (\text{ca. } 430\ \mathrm{nm}) \qquad (8b)$$

The resulting first-order rate constants, as given by the slopes of ln $[HCCO]_t$ versus *t* plots, are plotted in Figure 5 as a function of [NO] for three representative experimental temperatures. A weighted, least-squares linear fit to the data gives the second-order rate constant k_5. All experimental derivations of k_5 are listed in Table 1.

Like our previous measurements on the reaction of HCCO with O_2,[30] the second-order plots of Figure 5 have nonzero *y*-axis intercepts. Except for the different co-reactants, the initial chemical conditions for the two investigations are very similar. In both investigations, the intercepts are thought to be due to the fast reaction of HCCO with H atoms.[15] In our study of HCCO + O_2, most H atoms are coproduced with HCCO by the initial photolysis of CH_2CO. In the presence of NO however, additional H atoms are produced by the fast reaction NO + $CH_2(\tilde{X}) \rightarrow$ H + HCNO(isomer).[44−46] OH radicals, produced by the minor channel of this reaction, will be mainly removed by reaction with CH_2CO,[47] whereas a large fraction of H atoms will react with HCCO (as well as with CH_2 and CH_2CO). It is important therefore to ensure that the concentration of H atoms *over the time of* $[HCCO]_t$ *measurements*, $[H]_{av}$, is not appreciably different for experiments having different [NO]. Kinetic modeling[48] of the major reactions under our experimental conditions shows that for experiments at 296 K, $[H]_{av}$ increases from about 1.2×10^{13} cm^{-3} to about 2.0×10^{13} cm^{-3} over the [NO] range from 3.0×10^{14} cm^{-3} (lowest [NO]) to 1.4×10^{15} cm^{-3} (highest [NO]), respectively, and further, that this increase is due mainly to the reaction NO + $CH_2(\tilde{X})$. This change in $[H]_{av}$ has the effect of increasing the slope of the second-order plot by less than 3.0%. Indeed, at our highest NO concentration the removal of HCCO due to reaction with H is calculated to be about 3400 s^{-1} compared to a total measured removal rate of ca. 74 000 s^{-1}. This calculation assumes that every CH_2 produced in the photolysis of ketene is converted to H atoms via the CH_2 + NO reaction (using $k_{298K} = 3.8 \times 10^{-11}$ cm^3 s^{-1} $molecule^{-1}$ [49]). Although the above shows the contribution of HCCO removal by H atoms to be about 5% of the total removal, the percentage contribution on the overall rate constant is lower than this. This is because at our lowest concentration of NO at 298 K the contribution to the total observed removal rate of about 20 000 s^{-1} due to removal of HCCO by H is calculated to be 2100 s^{-1}. Thus there is only a weak [NO] dependence of the removal of HCCO by H atoms. The errors introduced by an increased $[H]_{av}$ with increasing [NO] in our

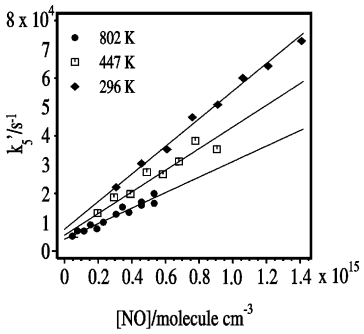

Figure 5. Variation of pseudo-first-order [HCCO] decay constants with [NO] at three reactor temperatures fitted to a function of the type $y = mx + c$ by a least-squares analysis.

TABLE 1: Experimental Absolute Rate Constants for the Reaction HCCO + NO at Various Temperatures

reactor temp (K)	$10^{11}k_5$ (cm^3 s^{-1} $molecule^{-1}$)
296	5.6 ± 0.5
296	5.7 ± 0.4
296	5.7 ± 0.4
296	5.3 ± 0.4
296	5.6 ± 0.5
296	4.8 ± 0.4
323	4.3 ± 0.3
345	4.6 ± 0.4
365	4.0 ± 0.4
396	3.5 ± 0.3
445	3.4 ± 0.3
447	3.5 ± 0.3
498	3.3 ± 0.3
558	3.3 ± 0.3
634	2.9 ± 0.3
638	2.6 ± 0.3
689	2.7 ± 0.2
802	2.7 ± 0.3

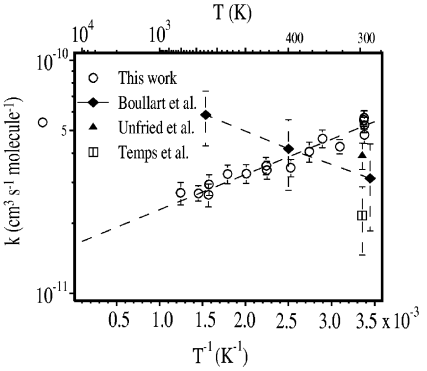

Figure 6. Experimental rate coefficients for HCCO + NO as a function of temperature plotted in Arrhenius form. The results of the present investigation (open circles) are fitted by a weighted, least-squares, analysis to a simple Arrhenius expression, yielding $k_5(T) = (1.6 \pm 0.2) \times 10^{-11}$ exp(340 ± 30 K/T) cm^3 s^{-1} molecule^{-1} (2σ errors). Also displayed are the only other direct experimental determinations of the rate constant for this reaction: the absolute rate determinations at room temperature by Unfried et al.[35] and Temps et al.,[36] and the relative-rate temperature-dependence study by Boullart et al.[10]

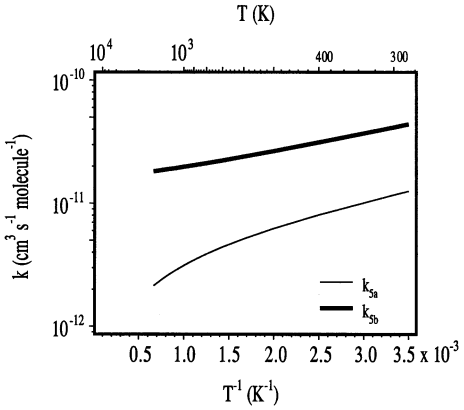

Figure 7. Calculated temperature dependence of the two main product channels of HCCO + NO, namely, HCN + CO (k_{5a}) and HNCO + CO (k_{5b}). These plots are derived from the present experimental measurements of $k_5(T)$, extrapolated to 2000 K, and the recent theoretical calculations of this laboratory on the ratio k_{5a}/k_{5b} (ref 40).

higher temperature measurements are slightly lower than that at room temperature, which is mainly due to decreased gas densities and therefore less initial radical production. These systematic errors, which are less than the random errors of individual determinations of k_5, are not corrected for, but simply added to the random errors.

The derived rate constants are plotted in Arrhenius form, together with previous determinations, in Figure 6. A weighted least-squares fit to the data gives $k_5(T) = (1.6 \pm 0.2) \times 10^{-11}$ exp(340 ± 30 K/T) cm^3 s^{-1} molecule^{-1} (2σ errors). The magnitude of the rate constant at room temperature is higher, but in reasonable agreement with the work of Unfried et al.,[35] and (within the broad overlapping uncertainties) with the work of Boullart et al.[10] The room-temperature determination of Temps et al.[36] lies lower than our determinations by a factor of approximately 2.

Unlike the only other determination of $k_5(T)$, a relative rate study that shows a slight positive temperature dependence,[10] the present results clearly show a decrease in rate constant with increasing temperature (although the k_5(400 K) determinations are in close agreement), and with no curvature detectable over the experimental temperature range. The reason for the discrepancy here is believed to be the temperature dependence of NO-catalyzed wall loss of O atoms in the former study.

The negative temperature dependence observed for this reaction is not unusual for a rapid barrier-less reaction between free radicals. A common explanation[50] is that the reaction takes place through the formation of a combination intermediate. The tightness of transition states leading to the formation of products forces the chemically activated intermediate to return to the reactant state as the system temperature is increased, because the higher energy transition state for re-dissociation is much looser. According to the theoretical work of Lin and co-workers,[51,52] this situation accounts entirely for the strong negative temperature dependence of the iso-electronic reaction NCO + NO.[53] Our recent theoretical work on the characterization of the HCCO + NO potential energy surface and calculations on the product branching ratios show that at 800 K the rate of re-dissociation of ON- -HCCO activated adduct is calculated to be approximately 5% of the isomerization reaction(s) leading to HCN + CO_2 and HCNO + CO. Allowing for possible errors, the rate of re-dissociation should be certainly less than 20% of isomerization. At 298 K re-dissociation should be totally negligible. A change in location of the entrance-channel (variational) transition state as the system temperature is increased must therefore be the dominant cause of the decrease in the rate constant.

Our previous calculations also show that the lifetimes of the chemically activated initial adducts and subsequent intermediates are all of the order of 10^{-12} s, such that there can be no pressure dependence either on the rate constant for HCCO + NO or on the product distribution below 100 bar.

Finally, combining the extrapolated k_5(T) obtained in the present work with the detailed RRKM calculations of this laboratory[40] on the branching ratio for this reaction, $k_{5a}/(k_{5a} + k_{5b}) = 0.0652 + 0.220$ exp(−T/917.9 K), and re-fitting to a modified Arrhenius function, gives the individual rate coefficients, from 296 to 2000 K, as $k_{5a} = (3.7 \pm 0.3) \times 10^{-10} T^{-0.72\pm0.02}$ exp(200 ± 30 K/T) cm^3 s^{-1} molecule^{-1} and $k_{5b} = (1.4 \pm 0.2) \times 10^{-11}$ exp(320 ± 30 K/T) cm^3 s^{-1} molecule^{-1}. The errors in k_{5a} and k_{5b} are derived only from the random errors associated with the present experimental results for the overall rate coefficient, k_5. The temperature dependences of k_{5a} and k_{5b} are plotted in Figure 7 and show the decreasing effectiveness with increasing temperature of HCN production and hence, in reburning environments, of NO removal by HCCO + NO. Indeed k_{5a} above is about a factor of 10 less (1200−1700 K) than that used in recent detailed chemical kinetic models of reburning.[12,13,39]

The experimental rate constants reported here agree in both magnitude and dependence on temperature with the very recent molecular-orbital/micro-variational RRKM calculations by Lin et al.,[54] which were made available to us during the review stage of this work. Their predicted total rate constant for this reaction is $k_5(T)_{calcd} = 2.27 \times 10^{-8} T^{-0.98}$ exp(−190 K/T) cm^3 s^{-1}.

4. Conclusions

The absolute rate constant of HCCO + NO has been, for the first time, experimentally determined over an extended temperature range. The precision of these data allows good extrapolation of the measured total rate constants to temperatures encountered in reburning conditions (up to 1700 K). These measurements, together with recent theoretical work of this laboratory on the product branching ratio, $k_{5a}/(k_{5a} + k_{5b})$, shows that the HCN-producing channel has a significant negative temperature dependence which also exhibits a downward curvature. This suggests that the dominance of the HCCO radical over other small, carbon-containing radicals in the removal of

NO in many reburning environments is less, and more sensitive to temperature, than previously assumed unless channel 5b, producing HCNO, is found to participate in reburning to a greater extent.

Acknowledgment. S.A.C. and L.V. gratefully acknowledge support of the Fund for Scientific Research, Flanders (FWO-Vlaanderen), each for a postdoctoral mandate and research project (PDM), and the KULeuven Research Council (BOF Fund) for continuing support. We thank Prof. M. C. Lin for supplying us with the results of micro-variational RRKM calculations on the HCCO + NO reaction prior to their publication.

Supporting Information Available: The detailed kinetic scheme used to determine the influence of secondary chemistry on the determination of k_5 is available free of charge via the Internet at http://pubs.acs.org.

References and Notes

(1) Grebe, J.; Homann, K. H. *Ber. Bunsen-Ges. Phys. Chem*. **1982**, *86*, 581.
(2) Grebe, J.; Homann, K. H. *Ber. Bunsen-Ges. Phys. Chem*. **1982**, *86*, 587.
(3) Devriendt, K.; Peeters, J. *J. Phys. Chem. A* **1997**, *101*, 2546.
(4) Peeters, J.; Devriendt, K. *Symp. (Int.) Combust. [Proc.]* **1996**, *26*, 1001.
(5) Marinov, N. M.; Pitz, W. J.; Westbrook, C. K.; Castaldi, M. J.; Senkan, S. M. *Combust. Sci. Technol*. **1996**, *21*, 116.
(6) McEnally, C. S.; Pfefferle, L. D. *Combust. Flame* **2000**, *121*, 575.
(7) Peeters, J.; Boullart, W.; Devriendt, K. *J. Phys. Chem*. **1995**, *99*, 3583.
(8) Phippen, D. E.; Bayes, K. D. *Chem. Phys. Lett.* **1989**, *164*, 625.
(9) Blauwens, J.; Smets, B.; Peeters, J. *Symp. (Int.) Combust. [Proc.]* **1976**, *16*, 1055.
(10) Boullart, W.; Nguyen, M. T.; Peeters, J. *J. Phys. Chem*. **1994**, *98*, 8036.
(11) Kilpinen, P.; Glarborg, P.; Hupa, M. *Ind. Eng. Chem. Res*. **1992**, *31*, 1477.
(12) Dagaut, P.; Luche, J.; Cathonnet, M. *Int. J. Chem. Kinet*. **2000**, *32*, 365.
(13) Dagaut, P.; Lecomte, F.; Chevailler, S.; Cathonnet, M. *Combust. Flame* **1999**, *119*, 494.
(14) Peeters, J. *Bull. Soc. Chim. Belg*. **1997**, *106*, 337.
(15) Vinckier, C.; Schaekers, M.; Peeters, J. *J. Phys. Chem*. **1985**, *89*, 508.
(16) Glass, G. P.; Kumaran, S. S.; Michael, V. J. *J. Phys. Chem. A* **2000**, *104*, 8360.
(17) Devriendt, K.; Van Poppel, M.; Boullart, W.; Peeters, J. *J. Phys. Chem*. **1995**, *99*, 16953.
(18) Peeters, J.; Vanhaelemeersch, S.; Van Hoeymissen, J.; Borms, R.; Vermeylen, D. *J. Phys. Chem*. **1989**, *93*, 3892.
(19) Butler, J. E.; Flemming, J. W.; Goss, L. P.; Lin, M. C. *Chem. Phys*. **1981**, *56*, 355.
(20) Vereecken, L.; Peeters, J. *J. Phys. Chem*. **1999**, *103*, 5523.
(21) Hack, W.; Koch, M.; Wagner, H. Gg.; Wilms, A. *Ber. Bunsen-Ges. Phys. Chem*. **1988**, *92*, 674.
(22) Canosa-Mas, C. E.; Ellis, M.; Frey, H. M.; Walsh, R. *Int J. Chem. Kinet*. **1988**, *16*, 1103.
(23) Miller, J. A.; Melius, C. F. *Combust. Flame* **1992**, *91*, 21.
(24) Boullart, W.; Devriendt, K.; Borms, R.; Peeters, J. *J. Phys. Chem.* **1996**, *100*, 998.
(25) Jones, I. T. N.; Bayes, K. D. *Symp. (Int.) Combust. [Proc.]* **1972**, *14*, 277.
(26) Schmoltner, A. M.; Chu, P. M.; Lee, Y. T. *J. Chem. Phys.* **1989**, *91*, 5365.
(27) (a) Peeters, J.; Schaekers, M.; Vinckier, C. *J. Phys. Chem*. **1986**, *90*, 6552. (b) Boullart, W.; Peeters, J. *J. Phys. Chem*. **1992**, *96*, 9810.
(28) Peeters, J.; Boullart, W.; Langhans, I. *Int. J. Chem. Kinet*. **1994**, *26*, 869.
(29) Michael, J. V.; Wagner, A. F. *J. Phys. Chem*. **1990**, *94*, 2453.
(30) Carl, S. A.; Sun, Q.; Peeters, J. *J. Chem. Phys*. **2000**, *114*, 10332.
(31) Wendt, J. O. L.; Sterling, C. V.; Matovich, M. A. *Symp. (Int.) Combust. [Proc.]* **1973**, *14*, 897.
(32) Kolb, T.; Jansohn, P.; Leuckel, W. *Symp. (Int.) Combust. [Proc.]* **1988**, *22*, 1193.
(33) Bowman, C. T. *Symp. (Int.) Combust. [Proc.]* **1992**, *24*, 859.
(34) Glarborg, P.; Alzueta, M. U.; Dam-Johansen, K.; Miller, J. A. *Combust. Flame* **1998**, *115*, 1.
(35) Unfried, K. G.; Glass, G. P.; Curl, R. F. *Chem. Phys. Lett*. **1991**, *177*, 33.
(36) Temps, F.; Wagner, H. Gg.; Wolf, M. *Z. Phys. Chem*. **1992**, *176*, 27.
(37) Eickhoff, U.; Temps, F. *Phys. Chem. Chem. Phys*. **1999**, *1*, 243.
(38) Rim, K. T.; Hershberger, J. F. *J. Phys. Chem. A* **2000**, *104*, 293.
(39) Miller, J. A.; Durant, J. L.; Glarborg, P. *Symp. (Int.) Combust. [Proc.]* **1998**, *27*, 235.
(40) Vereecken, L.; Sumathy, R.; Carl, S. A.; Peeters, J. *Chem. Phys. Lett*. **2001**, *344*, 400.
(41) Osborn, D. L.; Mordaunt, D. H.; Choi, H.; Bise, R. T.; Neumark, D. M.; Rohlfing, C. M. *J. Chem. Phys*. **1997**, *106*, 10087.
(42) Vaghjian, G. L. Work-in-progress, poster 4-D11, 28th International Symposuim on Combustion, Edinburgh, U.K., 2000.
(43) Pardon, A.; Peeters, J. *Rev. Sci. Instrum.* **1988**, *59*, 2499.
(44) Grussdorf, J.; Temps, F.; Wagner, H. G. *Ber. Bunsen-Ges. Phys. Chem*. **1997**, *101*, 134.
(45) Roggenbuck, J.; Temps, F. *Chem. Phys. Lett.* **1998**, *285*, 422.
(46) Su, H. M.; Kong, F. N.; Chen, B. Z.; Huang, M. B.; Liu, Y. J. *J. Chem. Phys.* **2000**, *113*, 1885.
(47) Oehlers, C.; Temps, F.; Wagner, H. G.; Wolf, M. *Ber. Bunsen-Ges. Phys. Chem*. **1992**, *96*, 171.
(48) Our model, in the absence of NO, is similar to that used by Glass et. al.[16] for modeling observed H atom concentrations, with the main exceptions being reactions 3, 7, 10, and 15−18 from that publication, which are omitted as they have no bearing on the present measurements. Although rate constants and product branching ratios for many reactions resulting from the addition of NO still have large uncertainties, the assumption of the overwhelming dominance of the main H-producing reaction of $CH_2(\tilde{X}) + NO \rightarrow H +$ products in our model still has negligible effect on our derived HCCO + NO rate constants. The model used is supplied as Supporting Information.
(49) Fikri, M.; Meyer, S.; Roggenbuck, J.; Temps, F. *Faraday Discuss.* **2001**, *119*, 223 and references therein.
(50) Mozurkewich, M.; Benson, S. W. *J. Phys. Chem*. **1984**, *88*, 6429.
(51) Lin, M. C.; Yisheng, H.; Melius, C. F. *J. Phys. Chem*. **1993**, *97*, 9124.
(52) Zhu, R.; Lin, M. C. *J. Chem. Phys*. **2000**, *104*, 10807.
(53) Yin, J. D.; Jiunn-Shin, L.; Wang, N. S. *Int. J. Chem. Kinet*. **1995**, *27*, 1111.
(54) Tokmakov, I. V.; Moskaleva, L. V.; Paschenko, D. V.; Lin, M. C. *J. Phys. Chem. A*, submitted for publication.